

# Numerical Simulation of the Actuation System for the ALDF's Propulsion Control Valve

John J. Korte\*

NASA Langley Research Center, Hampton, Virginia 23665

A numerical simulation of the actuation system for the propulsion control valve (PCV) of NASA Langley Aircraft Landing Dynamics Facility (ALDF) was developed during the preliminary design of the PCV and was used throughout the entire project. The numerical simulation is based on a predictive model of the PCV that was used to evaluate and design the unique actuation system. The PCV is a one-of-a-kind valve that controls a 1.7-million-lb thrust water jet used in propelling a 108,000-lb test carriage. The PCV can open and close in 0.300 s and deliver over 9000 gal of water per second at pressures up to 3150 psi. The actuation system of the PCV is a complicated mechanical-fluid power system designed for moving large masses at a high rate of acceleration. The design concept for the PCV was unique and it was built without the benefit of prototypes to verify the engineering design. The results of the numerical simulation of the PCV were used to predict transient performance and valve opening characteristics, specify the hydraulic control system, define transient loadings on components, and evaluate failure modes. The unique actuation system operated as the design intended and met the required performance without modification, largely because the results of the numerical simulation determined the required engineering parameters used to design the PCV. The mathematical model used for numerically simulating the mechanical fluid power system is described. Numerical results are demonstrated for a typical opening and closing cycle of the PCV. The computed results are shown to agree well with operational measurements. Finally, a summary is given on how the model was used in the design process. This paper demonstrates the advantages of having a predictive model for designing a complicated mechanical-fluid power system.

## Nomenclature

$A-F$	= linkage pins
$[A-F]_{x,y}$	= $x$ and $y$ components of pin reactions
$A_{gas_i}$	= effective gas piston area of cylinder $i$
$A_{oil_i}$	= effective oil piston area of cylinder $i$
$cv$	= valve flow coefficient
$I_i$	= moment of inertia about pin $i$ , $mR_g^2$
$I_{ij}$	= moment of inertia of link $ij$ , $m(L^2 + 3R_L^2)/12$
$k$	= spring constant
$L_{ij}$	= length between pins $i$ and $j$
$m$	= mass
$P_{gas_i}$	= gas pressure of cylinder $i$
$P_{oil_i}$	= oil pressure of cylinder $i$
$P_x$	= force output of dual cylinder into mechanism
$Q$	= oil volumetric flow rate
$R_{cg}$	= radius to center of gravity
$R_g$	= radius of gyration
$R_L$	= radius of linkage, 3 in.
$S_{1-4}$	= end of travel reactions inside dual cylinder
$T$	= torque
$t$	= time
$V_{gas_i}$	= gas volume of cylinder $i$
$V_{oil_i}$	= oil volume of cylinder $i$
$W$	= weight
$x, y$	= absolute coordinate positions
$x_{1,2}$	= piston position of opening, closing cylinder
$z$	= state vector

$\alpha_{ij}$	= counter clockwise angle from the horizontal to $ij$
$\beta$	= bulk modulus of oil
$\gamma$	= ratio of specific heats
$\Delta x_{ij}$	= difference in $x$ between pins $i$ and $j$
$\Delta y_{ij}$	= difference in $y$ between pins $i$ and $j$
$\delta$	= fraction of full opening, 0-1
$\eta$	= efficiency of cylinder
$\theta$	= shutter angle

## Introduction

MATHEMATICAL models, experiments, and analytical techniques are used to determine the requirements for engineering designs so that they will meet performance goals and operate safely. Design parameters for complicated mechanical systems that experience high accelerations are often based on scaling up the results obtained from testing prototypes. A high-acceleration unique mechanical fluid power actuation system was proposed for opening and closing the propulsion control valve (PCV) of NASA Langley Aircraft Landing Dynamics Facility (ALDF). The subject addressed by this paper is the numerical simulation developed to determine the design parameters for this unique actuation system.

The PCV was part of a project to increase the capability of ALDF.<sup>1</sup> The ALDF (Fig. 1) is a unique facility for the development and testing of aircraft and spacecraft landing gear systems.<sup>2</sup> In addition, the facility has been modified for testing airfoil performance in simulated rain.<sup>3</sup> A 108,000-lb carriage containing the landing gear or airfoil to be tested is propelled to speeds of up to 220 kt (170 kt with an airfoil) by an 18-in. diam jet of water. Approximately 26,000 gal of water are stored in an "L"-shaped vessel at pressures of up to 3150 psi. A maximum of 10,000 gal of water is released through the exit nozzle of the L-vessel during a test. The PCV covers the exit nozzle of the L-vessel and is used to control the flow of water through it. The PCV can open and close in 0.300 s and deliver over 9000 gal of water per second. The opening time and characteristic of the PCV govern the maximum loading on the carriage from the water jet. Therefore, both the opening

Presented as Paper 90-0079 at the AIAA 28th Aerospace Sciences Meeting, Reno, NV, Jan. 8-11, 1990; received Jan. 20, 1990; revision received Sept. 1, 1990; accepted for publication Oct. 20, 1990. Copyright © 1990 by the American Institute of Aeronautics and Astronautics, Inc. No copyright is asserted in the United States under Title 17, U.S. Code. The U.S. Government has a royalty-free license to exercise all rights under the copyright claimed herein for Governmental purposes. All other rights are reserved by the copyright owner.

\*Research Scientist, Theoretical Flow Physics Branch, Fluid Mechanics Division, Mail Stop 156. Member AIAA.

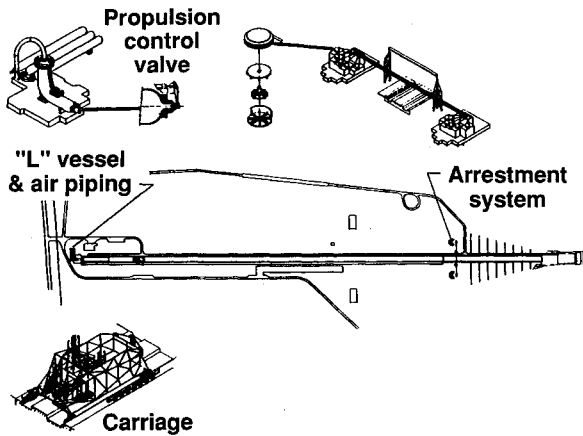


Fig. 1 Aircraft Landing Dynamics Facility (ALDF).

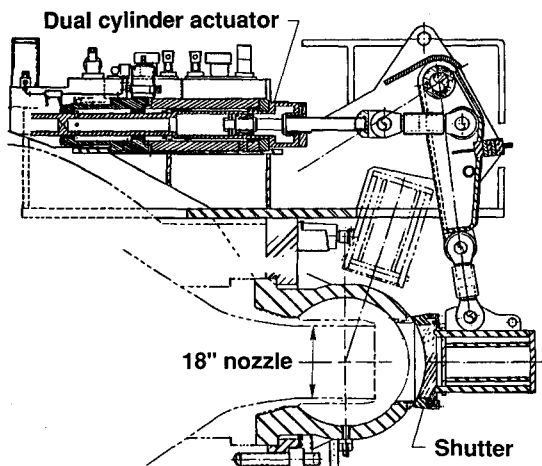


Fig. 2 Propulsion control valve (PCV).

time and characteristic of the PCV were specified to limit the loading on the carriage to under 17 g.

The PCV is a 20-in. spherical shaped shutter valve (Fig. 2). Two shutters are used, an interior shutter for primary seal and an exterior high-speed shutter (HSS) for controlling the water jet. Both shutters pivot about the geometric center of the partial spherical valve body. The investigation of the dynamics of the HSS actuation system is the purpose of the numerical simulation. The actuation system of the PCV is a complicated mechanical-fluid power system designed for moving large masses at a high rate of acceleration. The HSS is part of a four-bar linkage system (Fig. 3) connected to a special dual cylinder actuator (Fig. 4) using an offset slider-crank mechanism. The dual cylinder consists of two separate cylinder compartments each charged with nitrogen gas on one side of the piston and hydraulic oil on the opposite side of the piston (Fig. 4). All of the nitrogen gas (energy) necessary for operating the cylinders is located inside each cylinder. A set of hydraulic solenoid valves is used to release the oil from each cylinder and to initiate the opening or closing of the PCV (Fig. 5). Different opening times for the PCV are accomplished by adjusting a restriction in the hydraulic dump line. The above HSS system will be referred to as the actuation system for the PCV. The actuation system was required to open the PCV in a repeatable manner by maintaining the angular velocity of the shutter within prescribed limits without using a closed-loop control system. Closed-loop control for the HSS velocity or position could not be used due to the possibility of failure of the control system, which could damage the test carriage. The lack of a closed-loop control system required that the characteristics of the actuation system be known in sufficient detail

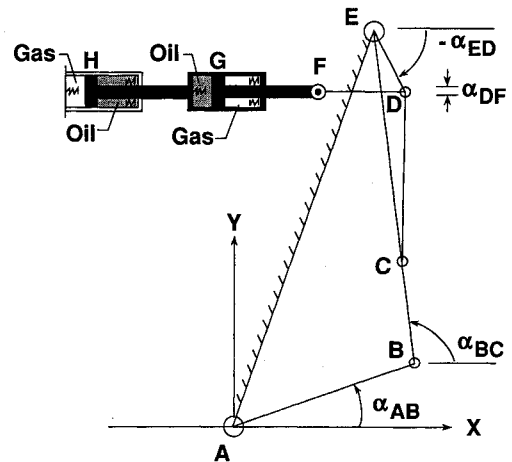


Fig. 3 Planar mechanism.

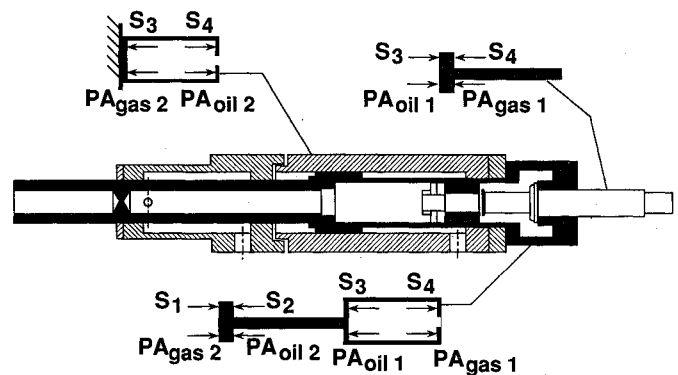


Fig. 4 Dual cylinder.

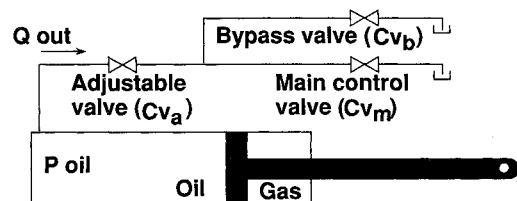


Fig. 5 Hydraulic valves.

to ensure that the desired performance would be obtained. Due to project schedule time constraints, a prototype of the actuation system for the PCV could not be built. Therefore, a predictive model<sup>4</sup> of the actuation system was developed that could be used to determine the necessary design parameters for the actuation system.

The initial design of the PCV was based on solving the kinematics and dynamics of the mechanism and actuator by graphical and manual calculations.<sup>5</sup> To accurately predict the transient behavior of the actuation system, the dynamics of the planar mechanism, the dual actuator, and the hydraulic controls have to be considered as a coupled system. In this paper, a mathematical model of the planar mechanism, dual actuator, and hydraulic controls is developed. The model is used to simulate a typical PCV opening/closing cycle, and comparisons are made with operational data. The analysis includes the kinematics and dynamics of the planar mechanism, including travel limits and joint friction, the dynamics of the dual actuator, including travel limits, the determination of nitrogen gas and oil pressures inside the dual actuator, including oil compressibility effects, and the oil control valve opening characteristics.

### Mathematical Model of the PCV

The components considered in the mathematical model of the actuation system for the PCV are shown in Fig. 6. The appropriate physical characteristics of the actuation system are given in Tables 1-4 for the pin locations shown in Fig. 3. The rotation of the HSS is defined by  $\theta$ , the location of the opening cylinder is  $x_1$ , and the location of the closing cylinder is  $x_2$ . The linkages are assumed to be rigid. The rotation ( $\theta$ ) of the HSS shutter can be directly related to the location ( $x_1$ ) of the opening cylinder through the kinematic equations for the mechanism. Therefore, the location of the opening ( $x_1$ ) and closing ( $x_2$ ) cylinders can be determined by solving a two-degree-of-freedom system.

### Kinematic Equations

The kinematic equations for the four-bar and slider-crank mechanism are determined using the constraint<sup>6</sup> approach. The equations for the pin positions of the mechanism can be determined from the geometric relationships. The appropriate relationships for the four-bar and slider-crank mechanism are (referring to Fig. 3)

$$x_B = L_{AB} \cos \alpha_{AB} \quad (1a)$$

$$y_B = L_{AB} \sin \alpha_{AB} \quad (1b)$$

$$x_C = x_E + L_{EC} \cos \alpha_{EC} \quad (1c)$$

$$y_C = y_E + L_{EC} \sin \alpha_{EC} \quad (1d)$$

$$x_D = x_E + L_{ED} \cos \alpha_{ED} \quad (1e)$$

$$y_D = y_E + L_{ED} \sin \alpha_{ED} \quad (1f)$$

$$x_F = x_D - L_{DF} \cos \alpha_{DF} \quad (1g)$$

$$L_{AB}^2 = x_B^2 + y_B^2 \quad (1h)$$

$$L_{BC}^2 = \Delta x_{BC}^2 + \Delta y_{BC}^2 \quad (1i)$$

$$L_{EC}^2 = \Delta x_{EC}^2 + \Delta y_{EC}^2 \quad (1j)$$

Given that the position of pin C is known, the location of pin B can be determined by solving the above system of nonlinear equations using either a Newton-Raphson iterative method<sup>7</sup> or, for a four-bar mechanism, a quadratic equation.<sup>6</sup> The equations for the velocity components of the different pins are determined by differentiation of Eq. (1), and a second differentiation gives the acceleration components.

### Equations of Motion for the Mechanism

The equations of motion for the mechanism are determined using the direct application of Newton's law of motion. The

direct method for determining the dynamical equations is used instead of the Lagrange's approach, since it is desired to determine the pin reactions as part of the solution procedure. For each linkage element, the effect of the inertial acceleration and gravity are included. The forces and moments are summed on each linkage component:

$$m_{C_{y1}} \ddot{x}_F = P_x - F_x \quad (2a)$$

$$\frac{1}{2} m_{DF} (\ddot{x}_D + \ddot{x}_F) = F_x - D_x \quad (2b)$$

$$\frac{1}{2} m_{DF} (\ddot{y}_D + \ddot{y}_F) = F_y - D_y - W_{DF} \quad (2c)$$

$$\frac{1}{2} m_{BC} (\ddot{x}_B + \ddot{x}_C) = C_x - B_x \quad (2d)$$

$$\frac{1}{2} m_{BC} (\ddot{y}_B + \ddot{y}_C) = C_y - B_y - W_{BC} \quad (2e)$$

$$I_A \ddot{\alpha}_{AB} = L_{AB} (B_x \sin \alpha_{AB} + B_y \cos \alpha_{AB}) - R_{c_{gA}} W_{AB} \cos \theta - T_{FRIC} - T_{SHOCK} \quad (2f)$$

$$I_{BC} \ddot{\alpha}_{BC} = \frac{1}{2} L_{BC} [(C_x + B_x) \sin \alpha_{BC} + (C_y + B_y) \cos \alpha_{BC}] \quad (2g)$$

$$I_{DF} \ddot{\alpha}_{DF} = \frac{1}{2} L_{DF} [(D_x + F_x) \sin \alpha_{DF} - (D_y + F_y) \cos \alpha_{DF}] \quad (2h)$$

$$I_E \ddot{\alpha}_{EC} = -L_{ED} (D_x \sin \alpha_{ED} + D_y \cos \alpha_{ED}) + L_{EC} (C_x \sin \alpha_{EC} + C_y \cos \alpha_{EC}) + R_{c_{gE}} W_{CDE} \cos [(\alpha_{ED} + \alpha_{EC})/2] - T_{BUMPER} \quad (2i)$$

The moments and acceleration are computed at the centroid of the linkage bars DF and BC. The angular acceleration for the

Table 1 Mechanism data

Link	Length, in.	Weight, lb.
A-B	34.004	5188
B-C	18.000	173
C-E	42.000	457
D-E	12.000	n.a.
D-F	20.000	178
F-G	35.000	155
G-H	n.a.	450

Table 2 Fixed points

Pin	X, in.	Y, in.
A	0.000	0.000
B	24.000	70.964
F	n.a.	60.572

Table 3 Crank data

	A-B	E-D-C
Radius gyration, in.	23.600	20.500
CG radius, in.	20.360	14.000
Stop radius, in.	32.000	27.000
Stop impact angle, deg	67.0	23.0
Link connection angle, deg	n.a.	22.338

Table 4 Actuator data (ready-to-fire)

	Open cylinder	Close cylinder
Gas pres., psi	3250	900
Gas piston, in. <sup>2</sup>	11.339	26.500
Gas vol., in. <sup>3</sup>	260.26	205.81
Oil piston, in. <sup>2</sup>	19.635	14.500
Oil vol., in. <sup>3</sup>	825.00	225.00
Stroke, in.	13.00	13.00

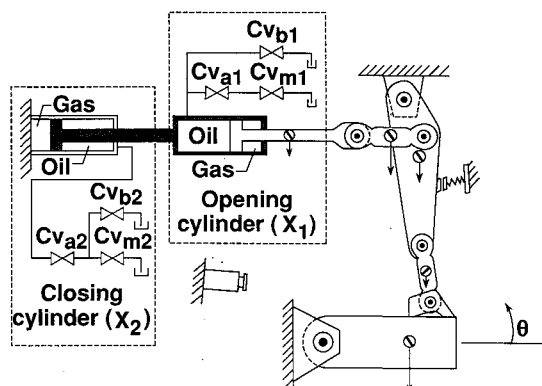


Fig. 6 Model of the propulsion control valve.

cranks AB and CED are computed about the fixed points A and E, respectively. The torque generated by friction, the shock absorber, and rubber bumper stop are designated as  $T_{FRIC}$ ,  $T_{SHOCK}$ , and  $T_{BUMPER}$ , respectively.

The travel of the linkage is limited by two identical shock absorbers in the open position and a rubber bumper in the closed position. The rubber bumper is simulated as a nonlinear spring. The variable orifice shock absorber is simulated as a nonlinear damper. The water pressure produces a huge force ( $\sim 1.3$  million lbf) on the HSS shutter, which is reacted through its center of rotation (pin A). The pressure force on the HSS drops to zero as the projected area of the HSS moves out of the water stream during the PCV opening. This large force develops a significant frictional torque about pin A during the opening of the valve. Spherical bearings are used at pin A that have a 6.9-in. radius and a coefficient of friction of 0.0025.

#### Equation of Motion for the Dual Cylinder

The dual cylinder develops the required force to open and close the PCV. One cylinder is used for opening and the second for closing. Each piston is driven by compressed nitrogen gas stored inside the cylinder. The piston is held in the firing position by high-pressure oil. When the fire command is received, a solenoid valve opens, releasing the oil into a reservoir. The oil pressure in the cylinder drops to the pressure generated by the oil flowing through an orifice. This process is very quick, resulting in a rapid increase in force applied to the piston.

The two cylinders are made to slide inside one another. To accurately represent the dynamics of the two cylinders, the load transfer through the structure has to be included. Consider the free body diagram (Fig. 4) for the two cylinders. The travel stops are simulated as stiff springs ( $S_{1-4}$ ), which have a stiffness based on the actual configuration. The force transferred into the linkage mechanism from the dual actuator is

$$P_x = \eta(P_{oil}A_{oil} - P_{gas}A_{gas})_{Cy1} + S_3 - S_4 \quad (3)$$

where the efficiency  $\eta$  is assumed to be 95%. Recall that the piston rod is directly connected to the linkage mechanism, so that the acceleration of the rod is considered in Eqs. (2). The equation of motion for the closing cylinder is

$$m_{Cy2}\ddot{x}_2 = \eta(P_{gas}A_{gas} - P_{oil}A_{oil})_{Cy2} - \eta(P_{oil}A_{oil} - P_{gas}A_{gas})_{Cy1} + S_1 - S_2 + S_3 - S_4 \quad (4)$$

The spring forces ( $S_{1-4}$ ) are zero unless the piston is at the beginning or the end of its stroke. The nitrogen pressures are calculated based on an isentropic expansion

$$P_{gas}(t) = P_{gas}(0)[V_{gas}(0)/V_{gas}(t)]^\gamma \quad (5a)$$

$$V_{gas1}(t) = V_{gas1}(0) - A_{gas1}[x_1(t) - x_1(0) - x_2(t) + x_2(0)] \quad (5b)$$

$$V_{gas2}(t) = V_{gas2}(0) + A_{gas2}[x_2(t) - x_2(0)] \quad (5c)$$

The rate of change of oil pressure is defined by

$$\dot{P}_{oil} = -\beta\dot{V}_{oil}/V_{oil} \quad (6a)$$

$$\dot{V}_{oil1} = (-\dot{x}_1 + \dot{x}_2)A_{oil1} - Q_{out1} \quad (6b)$$

$$\dot{V}_{oil2} = \dot{x}_2A_{oil2} - Q_{out2} \quad (6c)$$

$$V_{oil1}(t) = V_{oil1}(0) + A_{oil1}[x_1(t) - x_1(0) - x_2(t) + x_2(0)] \quad (6d)$$

$$V_{oil2}(t) = V_{oil2}(0) - A_{oil2}[x_2(t) - x_2(0)] \quad (6e)$$

where  $Q_{out}$  is the total volumetric oil flow rate through the solenoid valves.

#### Oil Control Valves

The movement of each cylinder in the dual actuator is initiated by opening the main and bypass control valves (Fig. 5). Different opening and closing times for the PCV are obtained by changing the setting ( $cv_a$ ) on the adjustable valves. Each cylinder is decelerated at the end of its stroke by closing the main control valve and throttling the remaining oil through the bypass valve.

The total volumetric oil flow rate is defined by

$$Q_{out} = \bar{cv}(P_{oil})^{1/2} \quad (7)$$

The effective valve flow coefficient is a function of the instantaneous opening of all the oil valves

$$\bar{cv} = [1/cv_a^2 + 1/(\delta_b cv_b + \delta_m cv_m)^2]^{-1/2} \quad (8)$$

The opening characteristic of the control valves is assumed to be sinusoidal. The opening and closing time of the control valves is adjustable. The fraction of opening ( $\delta$ ) of the control valves is specified as a function of time to obtain the desired PCV operation.

#### Numerical Procedure

The state of the system is obtained by the integration of six ordinary differential equations. The state vector  $z$  for the system is

$$z = [\dot{\alpha}_{EC}, \alpha_{EC}, \dot{x}_2, x_2, P_{oil1}, P_{oil2}]^T \quad (9)$$

A fourth-order Runge-Kutta algorithm is used to advance  $z$  in time. The initial conditions are obtained by determining the static equilibrium position of the linkage pins and cylinder pistons for the initial oil and gas pressures in the dual cylinder.

The derivative of  $z$  is determined as follows:

1) The oil flow out of the dual cylinder is computed using Eq. (7), and then the oil pressure derivatives are calculated with Eqs. (6).

2) The gas pressures and spring forces are calculated based on the cylinder's position, and then the acceleration of the closing cylinder is calculated with Eq. (4).

3) The force transfer into the linkage system is computed using Eq. (3), and then a linear system of equations is solved for the linkage system to determine the angular acceleration about crank CED.

The acceleration equations obtained from differentiating Eqs. (1) twice and the equations of motion given in Eqs. (2) described a linear system of equations for the pin reactions and linkage accelerations. Gaussian elimination is used to solve the sparse matrix equation to determine the forces and accelerations.

After each integration step, the new angular velocity and position about the crank CED are used to determine the linkage pin velocities and locations by solving the kinematic equations given by Eqs. (1).

#### Numerical Simulation of the PCV

The mathematical model presented above is used to numerically simulate the operation of the actuation system for the PCV. Two cases are presented. The first case simulates a typical opening and closing cycle of the PCV. The second case compares the numerical results to the operational measurements.

The first case simulates an opening of the PCV in 300 ms, followed by an 800-ms dwell, and a closing of the PCV in 310 ms. The opening time for the PCV is defined as the time starting with the development of flow area at the 20-in. exit and ending when the 18-in. jet is no longer impacted by the HSS.

The main oil control valve commands are programmed as shown in Fig. 7. The simulated response of the oil and gas pressures for the dual cylinder are shown in Figs. 8 and 9. The force output ( $P_x$ ) of the dual cylinder is shown in Fig. 10. The

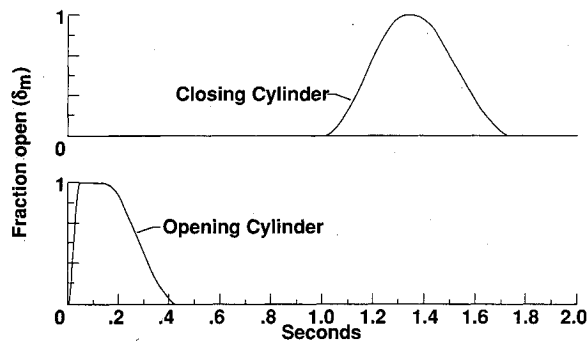


Fig. 7 Hydraulic control valve inputs.

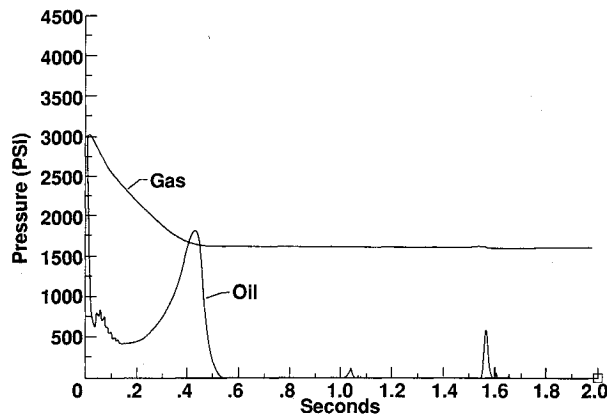


Fig. 8 Gas and oil pressure's response of opening cylinder.

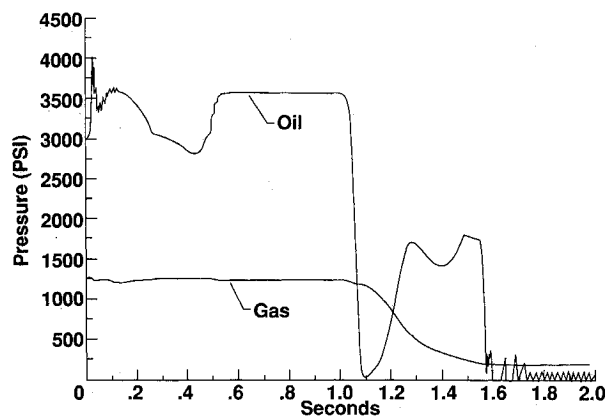


Fig. 9 Gas and oil pressure's response of closing cylinder.

positions and velocities of the cylinders are shown in Figs. 11 and 12. The compressed oil in the opening cylinder is released by the opening of  $cv_{m1}$ , resulting in a rapid drop in oil pressure and a large increase in  $P_x$ . The increase in force applied by the opening cylinder has to be transferred through the closing cylinder to the supports. This results in an increase in the closing cylinder's oil pressure during the opening stroke. The closing cylinder can be seen bouncing on the compressed oil column by the oscillation of the velocity trace. Towards the end of the opening stroke,  $cv_{m1}$  is closed, resulting in an increase in the opening cylinder's oil pressure that decelerates the mechanism. The opening cylinder comes to a hard stop against the closing cylinder at the end of the opening stroke.

The closing stroke is initiated by the opening of  $cv_{m2}$ . The closing cylinder oil pressure drops to zero until the cylinder begins to move. The large acceleration of the closing cylinder into the opening cylinder results in a slight oscillation of the

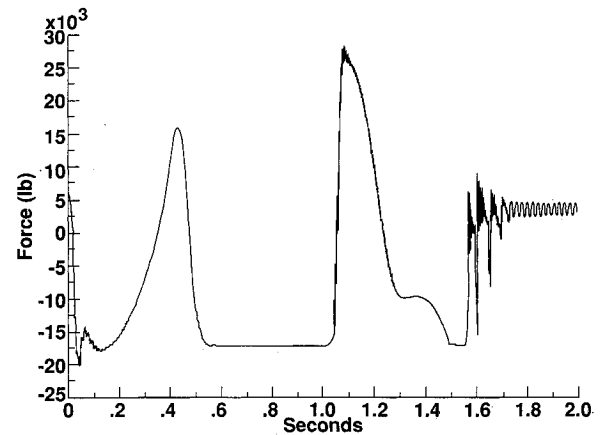


Fig. 10 Force developed by dual cylinder.

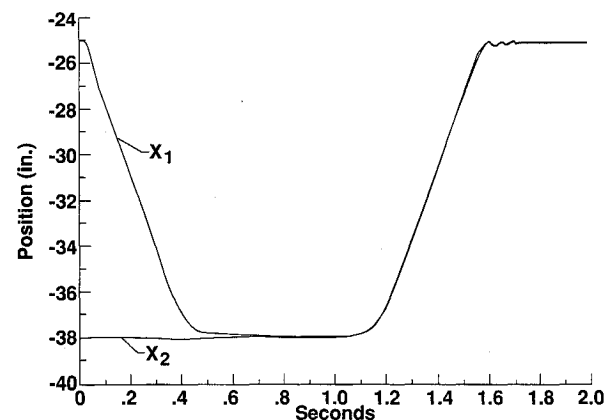


Fig. 11 Position of dual cylinder's piston.

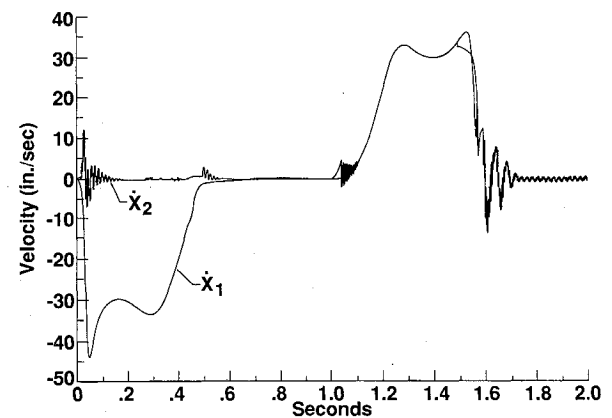


Fig. 12 Velocity of dual cylinder's piston.

velocities due to the bouncing of the closing cylinder into the opening cylinder. The two cylinders move as a unit during closing until  $cv_{m2}$  is closed and the deceleration of the mechanism is started. The deceleration force generated by the closing cylinder is greater than the force the opening cylinder can generate with the expanded gas in the cylinder. This is shown by the limit of  $P_x = -17,000$  lbf reached at 1.5 s. The opening and closing cylinders separate during the deceleration of the closing stroke, as shown by the changes in the velocities. The oscillation shown at the end of the closing stroke is the light bouncing of the crank CDE on the rubber stop.

The velocity and the position of the HSS are shown in Fig. 13. The opening and closing times for the PCV can be deter-

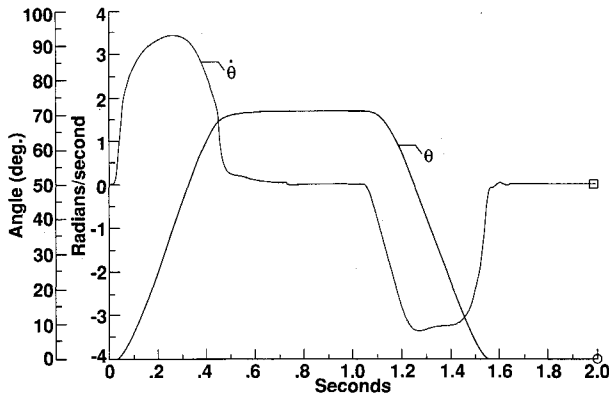


Fig. 13 Position and velocity of HSS.

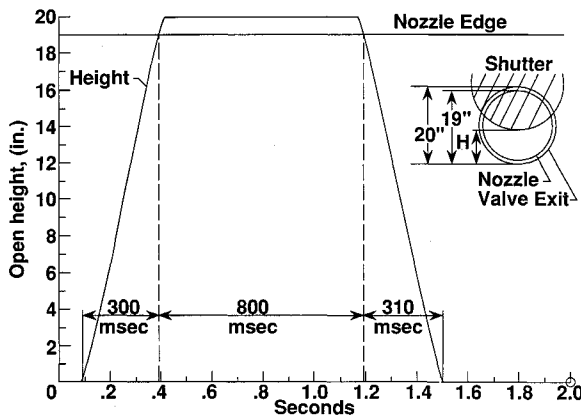


Fig. 14 Height of HSS.

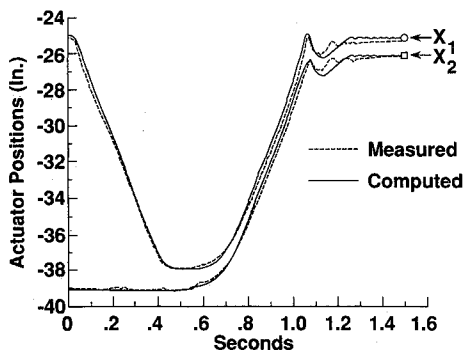


Fig. 15 Comparison of computed and measured piston positions.

mined by examining the height of the shutter (Fig. 14). The opening and closing times for the simulated case were a 300-ms opening, an 800-ms dwell, and a 310-ms closing.

#### Comparison with Operational Data

The initial checkout of the PCV required that the time history for the position of the opening and closing cylinders be recorded. A comparison of measurements of the opening and closing position of the dual cylinder was made with the pre-

dicted values from the simulation (Fig. 15). The mathematical model was updated to reflect the mass and inertia characteristics of the actual system. Excellent agreement is obtained between the prediction and the measurements.

#### Design Impact of Numerical Simulation

The results obtained from numerically simulating the actuation system for the PCV were used to specify design parameters. Six cases using both normal and failure operating conditions were simulated to define the maximum pin loadings for designing and analyzing the linkage elements. The investigation of the dynamics of the dual cylinder showed that the oil pressure could go as high as 4000 psi during the opening stroke and that the cylinders separated during the closing stroke. This required that the seals and the cylinders be evaluated for a higher design pressure than 3000 psi. The separation of the cylinders during the closing stroke was minimized by the recharging of the opening gas pressure during the closing stroke. The impact of the opening and closing cylinders was simulated for a zero dwell opening and failure of the main oil control valves. It was determined that the structural impact loads due to the two cylinders running into each other were excessive. An investigation was made that recommended the incorporation of a Belleville washer into the cylinder's design to minimize the impact loads. The sizes and operating times of the oil valves were determined by a study using the numerical simulation results. The control concept was also verified using the simulation.

#### Summary

A numerical simulation procedure has been developed for predicting the dynamics of the high-speed actuation system for the PCV. The equations used in the mathematical model were presented. A typical opening and closing cycle of the PCV was simulated and the dynamics were discussed. A comparison was made with operational measurements that showed good agreement. A brief summary was made of how the simulation was used in the design process and how it affected the final design. The unique actuation system operated as the design intended and met the required performance without modification, largely because the results of the numerical simulation determined the required engineering parameters used to design the PCV.

#### References

- <sup>1</sup>Davis, P. A., Stubbs, S. M., and Tanner, J. A., "Aircraft Landing Dynamics Facility, A Unique Facility with New Capabilities," Society of Automotive Engineers, SAE Paper 851938, Oct. 1985.
- <sup>2</sup>Davis, P. A., Stubbs, S. M., and Tanner, J. A., "Langley Aircraft Landing Dynamics Facility," NASA RP-1189, Oct. 1987.
- <sup>3</sup>Taylor, J. T., Moore, C. T., III, Campbell, B. A., and Melson, W. E., Jr., "The Development of a Facility for Full-scale Testing of Airfoil Performance in Simulated Rain," AIAA Paper 88-0055, Jan. 1988.
- <sup>4</sup>Paynter, H. M., and Shoureshi, R., "An Introduction to the Dynamics and Control of Thermofluid Processes and Systems," *Journal of Dynamic Systems, Measurement, and Control*, Vol. 107, Dec. 1985, pp. 230-232.
- <sup>5</sup>Dempsey, T., Reiner, T., and Gacs, P., "Dynamics Analysis for the Design of the Propulsion Valve Controls for the Aircraft Landing Simulator at NASA/Langley Research Center," S & Q Corporation Calculation Package, San Francisco, CA, Jan. 1983.
- <sup>6</sup>Molian, S., *Mechanism Design*, 1st ed., Cambridge Univ. Press, Cambridge, England, UK, 1982, pp. 106-118.
- <sup>7</sup>Paul, B., *Kinematics and Dynamics of Planar Machinery*, Prentice-Hall, Englewood Cliffs, NJ, 1979, pp. 300-304.